Mem. S.A.It. Vol. 86, 70

Memorie della

The expected very-high-energy flux from a population of globular clusters

C. Venter and A. Kopp**

Centre for Space Research, North-West University, Potchefstroom Campus, 2520 Potchefstroom, South Africa

Abstract. Given their old ages, globular clusters are expected to harbour many evolved stellar objects. Their high core densities enhance stellar encounter rates, also facilitating the formation of stellar end products. In particular, many millisecond pulsars are found in these clusters. Such a population of millisecond pulsars is expected to radiate several spectral components in the radio through γ-ray waveband. We present ongoing work involving a refined spectral model that assumes millisecond pulsars as sources of relativistic particles to model the multi-wavelength emission properties of globular clusters. We apply the model to a population of globular clusters that have been observed by H.E.S.S. and use upper limits derived from stacking analyses to test the viability of this "millisecond pulsar scenario". We derive general expressions for the ensemble-averaged flux and its error stemming from the uncertainty in free model parameters. The errors exceed this calculated average flux value so that there are regions in parameter space for which the model predictions satisfy the H.E.S.S. upper limits. Improved constraints on single-cluster parameters are therefore needed to aid in discriminating between competing spectral models.

Key words. Galaxy: globular clusters – Gamma rays: general – Radiation mechanisms: non-thermal

1. Introduction

Our Galaxy is home to ~160 globular clusters (GCs), each containing $N_* = 10^4 - 10^6$ stars (Harris 1996). They constitute a spherical distribution about the Galactic Centre, lying at an average distance $\langle d \rangle \sim 12$ kpc. GCs host exotic stellar systems such as black holes, white dwarfs, cataclysmic variables, and millisecond pulsars[1] (MSPs). This has been attributed to their old age (allowing stars to evolve to their end states) as well as dense cores (resulting in enhanced stellar encounter rates that facilitate formation of such systems); see, e.g., Pooley et al. (2003).

GCs radiate broadband spectra. For example, Terzan 5 has been detected in radio (Clapson et al. 2011), diffuse X-rays (Eger et al. 2010), GeV γ-rays (with the spectral characteristics pointing

** On leave from Institut für Experimentelle und Angewandte Physik, Christian-Albrechts-Universität zu Kiel, Leibnizstrasse 11, 24118, Kiel, Germany

[1] 28 of the ~160 known Galactic GCs contain 144 confirmed radio pulsars, the bulk of these being MSPs; *http://www.naic.edu/~pfreire/GCpsr.html*.

to the cumulative pulsed emission from a population of GC MSPs; Nolan et al. 2012), and in the TeV domain (Abramowski et al. 2011). Several spectral models have been proposed. Harding et al. (2005); Venter & de Jager (2008) calculated the total GeV contribution from GC MSPs by summing individual predicted pulsed curvature radiation spectra. In contrast, Cheng et al. (2010) assumed that the GeV emission was due to inverse Compton (IC) radiation by leptons escaping from the MSP magnetospheres, upscattering background photons. Earlier work by Bednarek & Sitarek (2007) considered MSPs that accelerate leptons either at the shocks that originate during collisions of neighbouring pulsar winds or inside the pulsar magnetospheres, followed by IC emission from these particles (see also Venter et al. 2009; Zajczyk et al. 2013 for updated calculations). Kopp et al. (2013) recently refined this model significantly, including a line-of-sight calculation of the X-ray surface brightness to constrain the diffusion coefficient. Another model by Bednarek (2012) assumed particle acceleration by non-accreting white dwarfs and predicted an observable γ-ray flux for the Cherenkov Telescope Array (CTA), depending on model parameters. Lastly, Domainko (2011) put forward a hadronic model invoking a γ-ray burst. Hadrons accelerated during a short burst may collide with ambient target nuclei, leading to π^0 particles that eventually decay into γ-rays.

To help discriminate between the various spectral models, we follow a population approach involving the calculation of an ensemble-averaged[2] spectrum, in order to reduce the uncertainty on the predicted spectrum. This is motivated by the stringent upper limits to the average single-GC TeV flux involving 15 non-detected GCs, obtained by the High Energy Stereoscopic System (H.E.S.S.; Abramowski et al. 2013). These upper limits are lower than the flux predicted by a simple leptonic scaling model by a factor of $\sim 3-30$, calling the leptonic models that invoke MSPs as sources of relativistic particles (the "MSP scenario") into question. We have made a first attempt to obtain improved estimates of the ensemble-averaged TeV flux (Venter & Kopp 2015a). This paper is a next step in the process to assess the plausibility of the MSP scenario. We describe our first results in Section 2, improved calculations in Section 3, and our conclusions in Section 4. Various mathematical results are given in Appendix A.

2. A first estimate of the ensemble-averaged flux involving 15 GCs

We applied our basic GC model (Kopp et al. 2013) to the 15 GCs that were not detected by H.E.S.S., fixing the parameters of each cluster to reasonable values (see Venter & Kopp 2015a for details). We found that none of the single-cluster spectra violate the TeV upper limits. Our ensemble-averaged single-GC flux is also below the upper limits for the given parameter choices. We found that the predicted spectra are quite sensitive to the choice of diffusion coefficient. Different energy dependencies lead to changes in the spectral shape, while a diffusion coefficient larger than the Bohm value may further lower the predicted flux.

3. New Results

We next performed a rigorous assessment of the error on the ensemble-averaged integral flux spectrum, simply due to uncertainty in the free (but constrained) GC parameters. We considered the following free parameters: distance d, number of stars in the GC N_*, index Γ of the injection spectrum, number of MSPs $N_{\rm MSPs}$, average particle conversion efficiency η, average MSP spin-down luminosity $\langle \dot{E} \rangle$, and cluster magnetic field B. We fix the minimum and maximum energies

[2] This term is taken to indicate the average of the summed spectra (i.e., the cumulative spectrum) involving all clusters in the population, for all possible values of single-cluster free parameters on a grid spanning reasonable values for the latter, divided by the number of GCs G. Thus, each of the unique parameter combinations may be thought of as a particular 'state' (or population instance), yielding a particular cumulative spectrum, and we average over all such states, after which we divide by G.

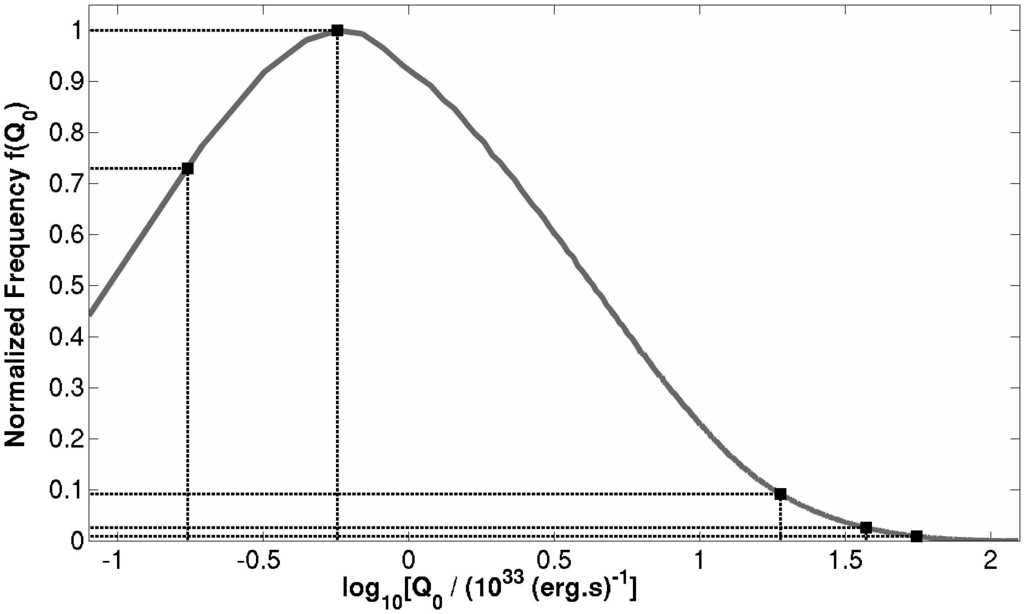

Fig. 1. Histogram of Q_0 obtained when considering reasonable ranges for $N_{\rm MSP}$, η, and $\langle \dot{E} \rangle$.

of the injection spectra, assume Bohm diffusion, and ignore the contribution of Galactic background photons to the IC flux (since these GCs have *a priori* been selected to lie off the Galactic Plane; Abramowski et al. 2013). For more details, see Venter & Kopp (2015b).

The 7 free model parameters however lead to a prohibitively large number of combinations (e.g., 15 GCs and 5 values per free parameter give $(5^7)^{15} \sim 10^{73}$ combinations). However, by investigating the ranges of the three parameters $N_{\rm MSPs}$, η, and $\langle \dot{E} \rangle$, we could combine these into a single source strength parameter (injection spectrum normalisation) Q_0, reducing the number of free parameters to 5. This parameter, however, does not follow a flat distribution (see Figure 1), and so one needs to carefully weight the contribution of single-GC spectra when calculating the final spectrum. We assessed the ensemble-averaged spectrum $\langle F \rangle / G$ and deviation σ / G by constructing single-GC spectra for all possible parameter combinations and dividing by the number of GCs[3]. We derived analytical expressions for $\langle F \rangle_{GQ'}$ and $\sigma_{GQ'}$, involving G clusters and a non-uniform number of occurances for different values of Q_0, under the assumption that each 5-parameter combination occurs only once (see Section A.6).

Figure 2 shows our integral fluxes calculated for the full population (the average of all 15 GCs is the leftmost value in light grey region, while individual cases are indicated on the x-axis). H.E.S.S. upper limits for the point-source and extended analyses are indicated by dashed and dash-triple-dotted lines (and dark grey backgrounds). We show the average fluxes (blue lines) as well as two error bands: orange and cyan lines indicate $\left(\langle F \rangle_{GQ'} + \sigma_{GQ'}\right)/G = \langle F \rangle_{GQ'} \left(1 + \sigma_{GQ'}/\langle F \rangle_{GQ'}\right)/G$ and $\langle F \rangle_{GQ'} \left(1 + \sigma_{GQ'}/\langle F \rangle_{GQ'}\right)^{-1}/G$; red and green lines indicate maximum and minimum integral fluxes (over all parameter combinations) at the H.E.S.S. values of the threshold energy $E_{\rm th}$. Although the average model flux violates the H.E.S.S. stacking

[3] For simplicity, we assume that each GC has been observed for the same period of time. Our results are not very different when taking into account different observing times (or 'live times') for each GC.

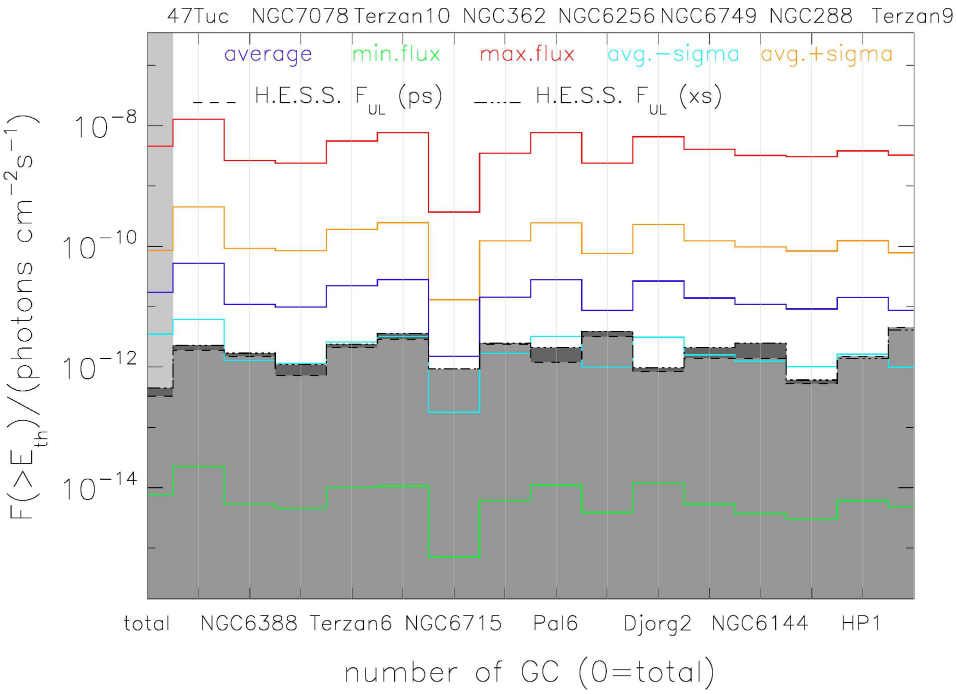

Fig. 2. Integral flux plotted for the ensemble-averaged flux ('total') as well as individual cases (as indicated on the *x*-axis). H.E.S.S. upper limits for the point-source (ps) and extended (xs) analyses are shown in dashed and dash-triple-dotted lines (and dark grey backgrounds). We indicate the average fluxes (blue line) as well as error bands. See text for details.

upper limits, we find that the errors on these fluxes are quite large. We should point out that $\langle F\rangle_{GQ'} - \sigma_{GQ'} \ll \langle F\rangle_{GQ'} \left(1 + \sigma_{GQ'}/\langle F\rangle_{GQ'}\right)^{-1}$, and since $\langle F\rangle_{GQ'} - \sigma_{GQ'} < 0$, we do not show this band on the logarithmic plot. Even though the lower error band (cyan line) underestimates the possible flux range, it is close to the H.E.S.S. upper limits for the single-GC cases. Moreover, there are indeed parameter combinations for which the ensemble-averaged integral flux is below the H.E.S.S. upper limit (e.g., the green line), given our assumptions for the number of free parameters as well as their ranges.

4. Conclusions

We have applied our refined GC model to a population of GCs. One important drawback is the uncertainty in model parameters, which translates into a large uncertainty on the final radiated spectra. We therefore followed a population approach, where we stacked spectra from several GCs in order to decrease the relative uncertainty in the ensemble-averaged spectrum. Although our average integral flux violates the H.E.S.S. upper limit, there are parameter combinations that yield fluxes below these limits. We expect the error band to widen if more parameters, such as the diffusion coefficient, are assumed free. We therefore need better (independent) constraints on single-GC parameters to discriminate between rival GC models.

Acknowledgements. This research is based on work supported by the South African National Research Foundation.

Appendix A: Mathematical results – averages and variances

We present details of the derivation of the cumulative GC flux and its 1σ deviation due to uncertainty in the parameters (in the paper, however, we need to divide by the number of clusters G to obtain the ensemble-averaged flux and its corresponding error). We assume that each parameter combination determining the cumulative spectrum occurs only once, i.e., we compute the GC spectra on a multivariate parameter grid, and then obtain the cumulative spectrum and variance.

Let f_{ng} be the single-GC spectrum of the g^{th} GC, corresponding to the n^{th} parameter combination, with $g = 1 \ldots G$, $n = 1 \ldots N$. Define the average spectrum of the g^{th} GC, averaged over N parameter combinations, by $\langle f_g \rangle = \frac{1}{N}\sum_{n=1}^{N} f_{ng}$.

A.1. CASE 1: Single cluster ($G = 1$), N parameter combinations, source strength Q_0 not considered separately

The average cumulative spectrum is given by

$$\langle F \rangle_1 = \langle f_1 \rangle = \frac{1}{N}\sum_{n=1}^{N} f_{n1}. \tag{A.1}$$

The variance is given by the well-known expression (using A.1)

$$\sigma_1^2 = \frac{1}{N-1}\sum_{n=1}^{N}\left(f_{n1} - \langle F \rangle_1\right)^2 \approx \frac{1}{N}\sum_{n=1}^{N}\left(f_{n1}^2 - 2 f_{n1}\langle F \rangle_1 + \langle F \rangle_1^2\right) = \langle f_1^2 \rangle - \langle f_1 \rangle^2. \tag{A.2}$$

A.2. CASE 2: Single cluster ($G = 1$), N parameter combinations, M source strengths Q_{0m}, each occuring with equal frequency

The single sum now becomes two nested sums, so that the average cumulative spectrum becomes

$$\langle F \rangle_Q = \frac{1}{MN}\sum_{m=1}^{M}\sum_{n=1}^{N} Q_{0m} f_{n1} = \frac{1}{M}\sum_{m=1}^{M} Q_{0m}\frac{1}{N}\sum_{n=1}^{N} f_{n1} = \langle Q_0 \rangle \langle f_1 \rangle. \tag{A.3}$$

Similarly,

$$\langle F^2 \rangle_Q = \frac{1}{MN}\sum_{m=1}^{M}\sum_{n=1}^{N}\left(Q_{0m} f_{n1}\right)^2 = \frac{1}{M}\sum_{m=1}^{M} Q_{0m}^2\frac{1}{N}\sum_{n=1}^{N} f_{n1}^2 = \langle Q_0^2 \rangle \langle f_1^2 \rangle. \tag{A.4}$$

The variance is calculated as

$$\begin{aligned}\sigma_Q^2 &\approx \frac{1}{M}\sum_{m=1}^{M} Q_{0m}^2\frac{1}{N}\sum_{n=1}^{N} f_{n1}^2 - 2\langle F \rangle_Q\frac{1}{M}\sum_{m=1}^{M} Q_{0m}\frac{1}{N}\sum_{n=1}^{N} f_{n1} + \langle F \rangle_Q^2 \\ &= \langle F^2 \rangle_Q - \langle F \rangle_Q^2 = \langle Q_0^2 \rangle \langle f_1^2 \rangle - \langle Q_0 \rangle^2 \langle f_1 \rangle^2. \end{aligned} \tag{A.5}$$

A.3. CASE 3: Single cluster ($G = 1$), N parameter combinations, M source strengths Q_{0m}, each occuring a different number of times w_m

Define $M' = \sum_{m=1}^{M} w_m$ and $\langle Q_0 \rangle' = \sum_{m=1}^{M} w_m Q_{0m}/M'$ as the weighted mean of Q_0. Then average cumulative spectrum becomes

$$\langle F \rangle_{Q'} = \frac{1}{M'N}\sum_{m=1}^{M}\sum_{n=1}^{N} w_m Q_{0m} f_{n1} = \frac{1}{M'}\sum_{m=1}^{M} w_m Q_{0m}\frac{1}{N}\sum_{n=1}^{N} f_{n1} = \langle Q_0 \rangle' \langle f_1 \rangle. \tag{A.6}$$

The average of the square of the cumulative flux becomes

$$\langle F^2\rangle_{Q'} = \frac{1}{M'N}\sum_{m=1}^{M}\sum_{n=1}^{N} w_m Q_{0m}^2 f_{n1}^2 = \frac{1}{M'}\sum_{m=1}^{M} w_m Q_{0m}^2 \frac{1}{N}\sum_{n=1}^{N} f_{n1}^2 = \langle Q_0^2\rangle'\langle f_1^2\rangle. \tag{A.7}$$

The variance is

$$\begin{aligned}
\sigma_{Q'}^2 &\approx \frac{1}{M'N}\sum_{m=1}^{M}\sum_{n=1}^{N} w_m\left(Q_{0m}f_{n1} - \langle F\rangle_{Q'}\right)^2 \\
&= \frac{1}{M'}\sum_{m=1}^{M} w_m Q_{0m}^2\frac{1}{N}\sum_{n=1}^{N} f_{n1}^2 - 2\langle F\rangle_{Q'}\frac{1}{M'}\sum_{m=1}^{M} w_m Q_{0m}\frac{1}{N}\sum_{n=1}^{N} f_{n1} + \langle F\rangle_{Q'}^2 \\
&= \langle F^2\rangle_{Q'} - \langle F\rangle_{Q'}^2 = \langle Q_0^2\rangle'\langle f_1^2\rangle - \left(\langle Q_0\rangle'\right)^2\langle f_1\rangle^2.
\end{aligned} \tag{A.8}$$

We see that $\langle Q_0\rangle$ in (A.5) is now replaced by $\langle Q_0\rangle'$, and $\langle Q_0^2\rangle$ by $\langle Q_0^2\rangle'$.

A.4. CASE 4: G clusters and N parameter combinations, Q_0 not considered separately

The average cumulative spectrum is

$$\begin{aligned}
\langle F\rangle_G &= \frac{1}{N^G}\underbrace{\sum_{n=1}^{N}\sum_{o=1}^{N}\ldots\sum_{s=1}^{N}}_{G\text{ sums}}(f_{n1} + f_{o2} + \ldots + f_{sG}) \\
&= \frac{1}{N^G}\sum_{n=1}^{N}\sum_{o=1}^{N}\ldots\sum_{s=1}^{N} f_{n1} + \frac{1}{N^G}\sum_{n=1}^{N}\sum_{o=1}^{N}\ldots\sum_{s=1}^{N} f_{o2} + \ldots + \frac{1}{N^G}\sum_{n=1}^{N}\sum_{o=1}^{N}\ldots\sum_{s=1}^{N} f_{sG} \\
&= \frac{1}{N^G}\sum_{n=1}^{N} f_{n1}\sum_{o=1}^{N}\ldots\sum_{s=1}^{N}[1] + \frac{1}{N^G}\sum_{o=1}^{N} f_{o2}\sum_{n=1}^{N}\ldots\sum_{s=1}^{N}[1] + \ldots + \frac{1}{N^G}\sum_{s=1}^{N} f_{sG}\sum_{n=1}^{N}\sum_{o=1}^{N}\ldots[1] \\
&= \frac{N^{G-1}}{N^G}\left[\sum_{n=1}^{N} f_{n1} + \sum_{o=1}^{N} f_{o2} + \ldots + \sum_{s=1}^{N} f_{sG}\right] = \sum_{g=1}^{G}\langle f_g\rangle.
\end{aligned} \tag{A.9}$$

The average of the square of the cumulative spectrum is

$$\begin{aligned}
\langle F^2\rangle_G &= \frac{1}{N^G}\underbrace{\sum_{n=1}^{N}\sum_{o=1}^{N}\ldots\sum_{s=1}^{N}}_{G\text{ sums}}(f_{n1} + f_{o2} + \ldots + f_{sG})^2 \\
&= \frac{1}{N^G}\sum_{n=1}^{N}\sum_{o=1}^{N}\ldots\sum_{s=1}^{N}\left(f_{n1}^2 + f_{o2}^2 + \ldots + f_{sG}^2\right) + \frac{2}{N^G}\sum_{n=1}^{N}\sum_{o=1}^{N}\ldots\sum_{s=1}^{N}\left(f_{n1}f_{o2} + f_{n1}f_{p3} + \ldots + f_{r,G-1}f_{sG}\right) \\
&= \frac{1}{N^G}\sum_{n=1}^{N} f_{n1}^2\sum_{o=1}^{N}\ldots\sum_{s=1}^{N}[1] + \frac{1}{N^G}\sum_{o=1}^{N} f_{o2}^2\sum_{n=1}^{N}\ldots\sum_{s=1}^{N}[1] + \ldots + \frac{1}{N^G}\sum_{s=1}^{N} f_{sG}^2\sum_{n=1}^{N}\sum_{o=1}^{N}\ldots[1] + \\
&+ \frac{2}{N^G}\left\{\sum_{n=1}^{N} f_{n1}\sum_{o=1}^{N} f_{o2}\ldots\sum_{s=1}^{N}[1] + \sum_{n=1}^{N} f_{n1}\sum_{p=1}^{N} f_{p3}\ldots\sum_{s=1}^{N}[1] + \ldots\right\}
\end{aligned}$$

$$= \frac{N^{G-1}}{N^G}\left\{\sum_{n=1}^{N} f_{n1}^2 + \sum_{o=1}^{N} f_{o2}^2 + \ldots + \sum_{s=1}^{N} f_{sG}^2\right\} + \frac{2N^{G-2}}{N^G}\left\{\sum_{n=1}^{N} f_{n1}\sum_{o=1}^{N} f_{o2} + \sum_{n=1}^{N} f_{n1}\sum_{p=1}^{N} f_{p3} + \ldots\right\}$$

$$= \sum_{g=1}^{G}\langle f_g^2\rangle + 2\sum_{g=1}^{G}\sum_{h=1,g<h}^{G}\langle f_g\rangle\langle f_h\rangle. \tag{A.10}$$

The variance is given by

$$\sigma_G^2 \approx \frac{1}{N^G}\sum_{n=1}^{N}\sum_{o=1}^{N}\ldots\sum_{s=1}^{N}\left(f_{n1} + f_{o2} + \ldots + f_{sG} - \langle F\rangle_G\right)^2$$

$$= \frac{1}{N^G}\sum_{n=1}^{N}\sum_{o=1}^{N}\ldots\sum_{s=1}^{N}\left(f_{n1} + f_{o2} + \ldots + f_{sG}\right)^2 - \frac{2}{N^G}\langle F\rangle_G\sum_{n=1}^{N}\sum_{o=1}^{N}\ldots\sum_{s=1}^{N}\left(f_{n1} + f_{o2} + \ldots + f_{sG}\right) + \langle F\rangle_G^2$$

$$= \langle F^2\rangle_G - \langle F\rangle_G^2 = \sum_{g=1}^{G}\sigma_g^2, \tag{A.11}$$

with σ_g indicating the standard deviation for each individual cluster g.

A.5. CASE 5: G clusters, N parameter combinations, M values for Q_0

It is now straightforward to generalise the previous case for the inclusion of another free parameter Q_0 which can take on M different values:

$$\langle F\rangle_{GQ} = \frac{1}{MN^G}\sum_{m=1}^{M}\underbrace{\sum_{n=1}^{N}\sum_{o=1}^{N}\ldots\sum_{s=1}^{N}}_{G\text{ sums}} Q_{0,m}\left(f_{n1} + f_{o2} + \ldots + f_{sG}\right) = \langle Q_0\rangle\sum_{g=1}^{G}\langle f_g\rangle = \langle Q_0\rangle\langle F\rangle_G. \tag{A.12}$$

$$\langle F^2\rangle_{GQ} = \frac{1}{MN^G}\sum_{m=1}^{M}\underbrace{\sum_{n=1}^{N}\sum_{o=1}^{N}\ldots\sum_{s=1}^{N}}_{G\text{ sums}} Q_{0,m}^2\left(f_{n1} + f_{o2} + \ldots + f_{sG}\right)^2$$

$$= \langle Q_0^2\rangle\sum_{g=1}^{G}\langle f_g^2\rangle + 2\langle Q_0^2\rangle\sum_{g=1}^{G}\sum_{h=1,g<h}^{G}\langle f_g\rangle\langle f_h\rangle = \langle Q_0^2\rangle\langle F^2\rangle_G. \tag{A.13}$$

$$\sigma_{GQ}^2 \approx \frac{1}{MN^G}\sum_{m=1}^{M}\underbrace{\sum_{n=1}^{N}\sum_{o=1}^{N}\ldots\sum_{s=1}^{N}}_{G\text{ sums}}\left[Q_{0,m}\left(f_{n1} + f_{o2} + \ldots + f_{sG}\right) - \langle F\rangle_{GQ}\right]^2$$

$$= \langle Q_0^2\rangle\sum_{g=1}^{G}\langle f_g^2\rangle + 2\langle Q_0^2\rangle\sum_{g=1}^{G}\sum_{h=1,g<h}^{G}\langle f_g\rangle\langle f_h\rangle - \langle Q_0\rangle^2\left[\sum_{g=1}^{G}\langle f_g\rangle\right]^2$$

$$= \langle F^2\rangle_{GQ} - \langle F\rangle_{GQ}^2 = \langle Q_0^2\rangle\langle F^2\rangle_G - \langle Q_0\rangle^2\langle F\rangle_G^2 \tag{A.14}$$

$$= \sigma_Q^2\left[\sum_{g=1}^{G}\langle f_g^2\rangle + 2\sum_{g=1}^{G}\sum_{h=1,g<h}^{G}\langle f_g\rangle\langle f_h\rangle\right] + \langle Q_0\rangle^2\sum_{g=1}^{G}\sigma_g^2, \tag{A.15}$$

with $\sigma_Q = \langle Q_0^2\rangle - \langle Q_0\rangle^2$.

A.6. CASE 6: G clusters, N parameter combinations, M values of Q_0, each occurring w_m times

The average cumulative spectrum is given by

$$\langle F\rangle_{GQ'} = \frac{1}{M'N^G}\sum_{m=1}^{M}\underbrace{\sum_{n=1}^{N}\sum_{o=1}^{N}\ldots\sum_{s=1}^{N}}_{G\text{ sums}} w_m Q_{0,m}\left(f_{n1}+f_{o2}+\ldots+f_{sG}\right) = \langle Q_0\rangle'\langle F\rangle_G. \tag{A.16}$$

Similarly, we have

$$\begin{aligned}\langle F^2\rangle_{GQ'} &= \frac{1}{M'N^G}\sum_{m=1}^{M}\underbrace{\sum_{n=1}^{N}\sum_{o=1}^{N}\ldots\sum_{s=1}^{N}}_{G\text{ sums}} w_m Q_{0,m}^2\left(f_{n1}+f_{o2}+\ldots+f_{sG}\right)^2 \\ &= \langle Q_0^2\rangle'\sum_{g=1}^{G}\langle f_g^2\rangle + 2\langle Q_0^2\rangle'\sum_{g=1}^{G}\sum_{h=1,g<h}^{G}\langle f_g\rangle\langle f_h\rangle = \langle Q_0^2\rangle'\langle F^2\rangle_G.\end{aligned} \tag{A.17}$$

Finally, this leads to the following variance

$$\begin{aligned}\sigma_{GQ'}^2 &= \frac{1}{M'N^G}\sum_{m=1}^{M}\underbrace{\sum_{n=1}^{N}\sum_{o=1}^{N}\ldots\sum_{s=1}^{N}}_{G\text{ sums}} w_m\left[Q_{0,m}\left(f_{n1}+f_{o2}+\ldots+f_{sG}\right)-\langle F\rangle_{GQ'}\right]^2 \\ &= \langle F^2\rangle_{GQ'} - \langle F\rangle_{GQ'}^2 \\ &= \sigma_{Q'}^2\left[\sum_{g=1}^{G}\langle f_g^2\rangle + 2\sum_{g=1}^{G}\sum_{h=1,g<h}^{G}\langle f_g\rangle\langle f_h\rangle\right] + \left(\langle Q_0\rangle'\right)^2\sum_{g=1}^{G}\sigma_g^2,\end{aligned} \tag{A.18}$$

with $\sigma_{Q'} = \langle Q_0^2\rangle' - \left(\langle Q_0\rangle'\right)^2$.

References

Abramowski, A. *et al.*, 2011, A&A, 531, L18
Abramowski, A. *et al.*, 2013, A&A, 551, A26
Bednarek, W., & Sitarek, J., 2007, MNRAS, 377, 920
Bednarek, W., 2012, Phys. G: Nucl. Part. Phys., 39, 065001
Cheng, K. S. *et al.*, 2010, ApJ, 723, 1219
Clapson A.-C., Domainko, W. F., Jamrozy, M., Dyrda, M., & Eger, P., 2011, A&A, 532, A47
Domainko, W. F., 2011, A&A, 533, L5
Eger, P., Domainko, W. F., & Clapson, A.-C., 2010, A&A, 513, A66
Harris, W. E., 1996, AJ, 112, 1487
Harding, A. K., Usov, V. V., & Muslimov, A. G., 2005, ApJ, 622, 531
Kopp, A., Venter, C., Büsching, I., & de Jager, O. C., 2013, ApJ, 779, 126
Nolan, P. L. *et al.*, 2012, ApJS, 199, 31
Pooley, D. *et al.*, 2003, ApJ, 591, L131
Venter, C., & de Jager, O. C., 2008, ApJ, 680, L125
Venter, C. *et al.*, 2009, ApJ, 696, L52
Venter, C., & Kopp, A. 2015a, Proc. SAIP2014, *submitted.*
Venter, C., & Kopp, A. 2015b, *in prep.*
Zajczyk, A., Bednarek, W., & Rudak, B., 2013, MNRAS, 432, 3462